JOURNAL OF MATERIALS SCIENCE **34** (1999) 5861–5869

Analytical modelling of mechanical properties for rubber-toughened polymers

QI-ZHI WANG
Beijing University of Aeronautics and Astronautics, Beijing, People's Republic of China
DONG-JOO LEE
Yeungnam University, Gyungsan, Gyungbuk, Korea
E-mail: djlee@ynucc.yeungnam.ac.kr

Using a new quasi-sphere model, an analytical method is presented to determine the material properties and stress concentration factors of rubber-toughened polymers. The calculation is simple and the closed form results fit quite well with experimental data and various results using the finite element method. This simple and efficient method can be easily used to calculate a huge amount of results to fit the requirement of engineering. Also, this type of modeling can provide a better understanding of deformation mechanisms for development of this important composite material.

1. Introduction

Certain types of polymeric material are relatively brittle, and are often toughened by adding rubber particles. The dispersion of rubber particles in the polymer matrix causes stress concentration. The mechanism of toughening, which is still a subject of controversy, can be mainly described in two aspects: one is shear yielding, or shear banding and the other is internal cavitation, or interfacial debonding [1–5]. It can be better understood by examination of stress concentration and distribution derived from a theoretical model.

There were few attempts to predict the mechanical properties of the rubber toughened materials [6–9] using a finite element method (FEM). In general, 3-D FEM is very complex and needs the many cells for this type of material with its stress concentration and complex structure. Recently, Chen and Mai have used a 3-D model to analyze this problem [10], but the element of their micromechanical model is not small, enough especially in regions where the stresses are comparatively large. The most commonly used model is an axisymmetric model [6–8], based on the assumption that the material consists of cylinders, and each contains a rubber sphere in the center. But, this model does not reflect the overall isotropy of the material, so the results are somewhat questionable. Also, a 2-D model is used [8] which is of course more suspicious.

A better statistical isotropic model is the sphere model, based on the assumption that the material consists of spheres, each containing a rubber sphere in the center. It is well known that composite spheres′ assemblage theory can be used to determine the bulk modulus of statistically isotropic composites, such as rubber-toughed polymers [11]. It's simple, but the detailed information such as stress concentration and other elastic properties are needed.

Therefore, the FEM method is used to give out the material properties of this composite material [9]. But, the result seems quite limited and sometimes inaccurate. One reason is, for statistically distributed and unique sized particles, even the best-packed spheres can only occupy 74% of the whole space in the unit cell. A complete neglect of the remaining 26%, or in another word, averaging them into spheres may cause a big difference in the experiment results [12, 13].

Using the sphere model, in this paper, an analytical method is presented to determine the material properties and stress concentration factors of the rubber-toughened polymers. The remaining 26% of the matrix is also considered, but simplified by two reasonable assumptions. So, this model can be called a quasi-sphere model. The calculations are simple and the results fit quite well with experiment results.

2. Principles

An axisymmetric sphere model is chosen, as shown in Fig. 1. In spherical coordinates the Laplace equation becomes [14]

$$\nabla^2\psi = \frac{1}{R^2}\frac{\partial}{\partial R}\left(R^2\frac{\partial\psi}{\partial R}\right) + \frac{1}{R^2\sin\varphi}\frac{\partial}{\partial\varphi}\left(\sin\varphi\frac{\partial\psi}{\partial\varphi}\right) + \frac{1}{R^2\sin^2\varphi}\frac{\partial^2\psi}{\partial\theta^2} = 0 \quad (1)$$

In an axisymmetric condition, ψ is independent of θ, it can be written by separation of variables as:

$$\Psi = AR^nP_n(\zeta) + B\frac{1}{R^n}P_n(\zeta) \quad (2)$$

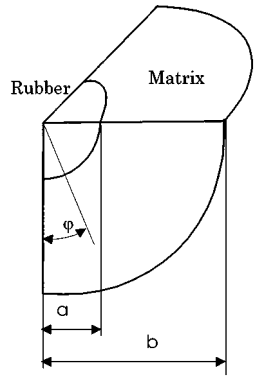

Figure 1 Spherical model.

where, $\zeta = \cos\varphi$ and $P_n(\zeta)$ is a Legendre polynomial of degree n, which satisfies the equation

$$(1-\zeta^2)\frac{d^2P_n(\zeta)}{d\zeta^2} - 2\zeta\frac{dP_n(\zeta)}{d\zeta} + n(n+1)P_n(\zeta) = 0 \tag{3}$$

By Rodrigues's formula, $P_n(\zeta)$ can be written as

$$P_n(\zeta) = \frac{1}{2^n n!}\frac{d^n(\zeta^2-1)^n}{d\zeta^n} \tag{4}$$

So, $P_0(\zeta)=1$, $P_1(\zeta)=\zeta$, $P_2(\zeta)=\frac{1}{2}(3\zeta^2-1)$, $P_3(\zeta)=\frac{1}{2}(5\zeta^3-3\zeta)$, $P_4(\zeta)=\frac{1}{8}(35\zeta^4-30\zeta^2+3)\ldots$

These polynomials form an orthogonal set across the region of $-1 \le \zeta \le 1$. A Papkovich-Neuber's solution of the Navier equations can be used. The displacement vector exclusive of body forces can be written as

$$\vec{u} = 4(1-\nu)\vec{B} - \vec{\nabla}(\vec{R}\cdot\vec{B} + B_0) \tag{5}$$

where $\vec{B}$ is a harmonic vector and B_0 is a harmonic function. In spherical coordinates, the displacements become:

$$u_R = 4(1-\nu)B_R - \frac{\partial}{\partial R}(RB_R + B_0), \quad u_\theta = 0$$

and

$$u_\varphi = 4(1-\nu)B_\varphi - \frac{1}{R}\frac{\partial}{\partial\varphi}(RB_R + B_0) \tag{6}$$

The following can be taken as the spherical components of a harmonic vector:

$$B_R = \sum_n R^{n+1}\{-A_n(n+1)P_n(\zeta) + \zeta P_{n+1}(\zeta)[A_n(n+1) + A'_{n+1}]\}$$

and

$$B_\varphi = -\sum_n R^{n+1}\{A_n P'_n(\zeta) + P_{n+1}(\zeta)[A_n(n+1) + A'_{n+1}]\}\sin\varphi \tag{7}$$

The harmonic function can be chosen as

$$B_0 = -\sum_n B_n R^n P_n(\zeta) \tag{8}$$

After substitution and simplification, we can get:

$$u_R = \sum_n \left[A_n(n+1)(n-2+4\nu)R^{n+1} + B_n n R^{n-1}\right]P_n(\zeta)$$
$$u_\varphi = \sum_n \left[A_n(n+5-4\nu)R^{n+1} + B_n R^{n-1}\right]\frac{d}{d\varphi}P_n(\zeta) \tag{9}$$

This is the general solution of the "interior problem" for an axisymmetrically loaded solid sphere. The solution of "exterior problem", or an axisymmetrically loading on a spherical hole in an infinite solid, can be obtained from the previous solution by replacing n with $-(n+1)$ but noting that $P_{-(n+1)} = P_n$. From this, we obtain

$$u_R = \sum_n \left[\frac{C_n}{R^n}n(n+3-4\nu) - \frac{D_n(n+1)}{R^{n+2}}\right]P_n(\zeta)$$
$$u_\varphi = \sum_n \left[\frac{C_n}{R^n}(-n+4-4\nu) + \frac{D_n}{R^{n+2}}\right]\frac{d}{d\varphi}P_n(\zeta) \tag{10}$$

For hollow sphere, it can be obtained that:

$$u_R = \sum_n \left[A_n(n+1)(n-2+4\nu)R^{n+1} + B_n n R^{n-1} + \frac{C_n}{R^n}n(n+3-4\nu) - \frac{D_n(n+1)}{R^{n+2}}\right]P_n(\zeta)$$
$$u_\varphi = \sum_n \left[A_n(n+5-4\nu)R^{n+1} + B_n R^{n-1} + \frac{C_n}{R^n}(-n+4-4\nu) + \frac{D_n}{R^{n+2}}\right]\frac{d}{d\varphi}P_n(\zeta) \tag{11}$$

Or, we can use a simplified form:

$$u_R = R\sum_n \bar{u}_R^n P_n(\zeta)$$
$$u_\varphi = R\sum_n \bar{u}_\varphi^n \frac{d}{d\varphi}P_n(\zeta) \tag{12}$$

where

$$\bar{u}_R^n = \bar{A}_n(n+1)(n-2+4\nu)\bar{R}^n + \bar{B}_n n\bar{R}^{n-2} + \frac{\bar{C}_n}{R^{n+1}}n(n+3-4\nu) - \frac{\bar{D}_n(n+1)}{R^{n+3}}$$
$$\bar{u}_\varphi^n = \bar{A}_n(n+5-4\nu)\bar{R}^n + \bar{B}_n\bar{R}^{n-2} + \frac{\bar{C}_n}{R^{n+1}}(-n+4-4\nu) + \frac{\bar{D}_n}{R^{n+3}}$$

and

$$\bar{R} = R/b, \quad \bar{A}_n = A_n b^n, \quad \bar{B}_n = B_n b^{n-2},$$
$$\bar{C}_n = C_n b^{-n-1}, \quad \bar{D}_n = D_n b^{-n-3}.$$

Then, the strains and stresses can be determined. The stresses become:

$$\frac{1}{2G}\sigma_{RR} = \sum_n \Big[A_n(n+1)(n^2-n-2-2\nu)R^n + B_n n(n-1)R^{n-2} - \frac{C_n}{R^{n+1}} n(n^2+3n-2\nu) + \frac{D_n(n+1)(n+2)}{R^{n+3}} \Big] P_n(\zeta) \quad (13)$$

$$\frac{1}{2G}\sigma_{R\varphi} = \sum_n \Big[A_n(n^2+2n-1+2\nu)R^n + B_n(n-1)R^{n-2} + \frac{C_n}{R^{n+1}}(n^2-2+2\nu) - \frac{D_n(n+2)}{R^{n+3}} \Big] \frac{d}{d\varphi} P_n(\zeta) \quad (14)$$

$$\frac{1}{2G}\sigma_{\varphi\varphi} = \sum_n \Big[-A_n(n+1)(n^2+4n+2+2\nu)R^n - B_n n^2 R^{n-2} + \frac{C_n}{R^{n+1}} n(n^2-2n-1+2\nu) - \frac{D_n(n+1)^2}{R^{n+3}} \Big] P_n(\zeta) + \sum_n \Big[A_n(n+5-4\nu)R^n + B_n R^{n-2} - \frac{C_n}{R^{n+1}}(-n+4-4\nu) - \frac{D_n}{R^{n+3}} \Big] ctg\varphi \frac{d}{d\varphi} P_n(\zeta) \quad (15)$$

$$\frac{1}{2G}\sigma_{\theta\theta} = \sum_n \Big[A_n(n+1)(n-2-2\nu-4n\nu)R^n + B_n n R^{n-2} + \frac{C_n}{R^{n+1}} n(n+3 - 2\nu - 4n\nu) - \frac{D_n(n+1)}{R^{n+3}} \Big] P_n(\zeta) + \sum_n \Big[A_n(n+5-4\nu)R^n + B_n R^{n-2} - \frac{C_n}{R^{n+1}}(-n+4-4\nu) - \frac{D_n}{R^{n+3}} \Big] ctg\varphi \frac{d}{d\varphi} P_n(\zeta) \quad (16)$$

We can also use another form:

$$\frac{1}{2G}\sigma_{RR} = \sum_n \bar{\sigma}^n_{RR} P_n(\zeta) \quad (17)$$

$$\frac{1}{2G}\sigma_{R\varphi} = \sum_n \bar{\sigma}^n_{R\varphi} \frac{d}{d\varphi} P_n(\zeta) \quad (18)$$

$$\frac{1}{2G}\sigma_{\varphi\varphi} = \sum_n \bar{\sigma}^n_{\varphi\varphi} P_n(\zeta) + \sum_n \bar{\sigma}^{n^*}_{\varphi\varphi} ctg\varphi \frac{d}{d\varphi} P_n(\zeta) \quad (19)$$

$$\frac{1}{2G}\sigma_{\theta\theta} = \sum_n \bar{\sigma}^n_{\theta\theta} P_n(\zeta) + \sum_n \bar{\sigma}^{n^*}_{\theta\theta} ctg\varphi \frac{d}{d\varphi} P_n(\zeta) \quad (20)$$

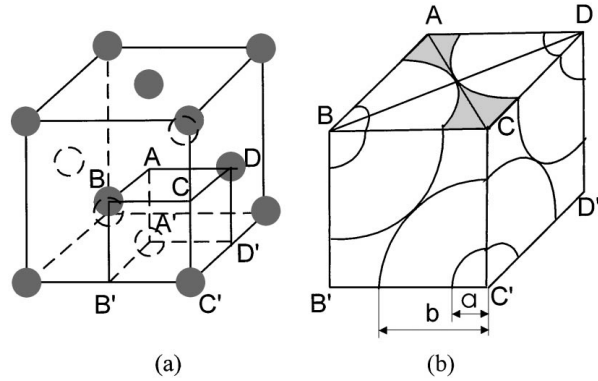

Figure 2 Micromechanical model.

Furthermore, we can choose a face-centered model as shown in Fig. 2a. Then, cut out a unit cell with four spheres to discuss as shown in Fig. 2b. Of course, the stresses and displacements of each sphere are not exactly axisymmetric. But, they can be taken as approximately axisymmetric when the volume fraction of the particles is not very large. Therefore, we can use the above theory.

As the sphere is symmetric with regard to the equator, n should be an even number. To simplify the situation, we choose n as equal to 0 and 2. So, there are 6 unknown parameters A_0, D_0, A_2, B_2, C_2, D_2, B_0 and C_0 that do not appear from the above formulas.

The boundary conditions must now be considered. First, we will discuss the boundary conditions of the rubber sphere.

(1) The Young's modulus of the rubber sphere is much smaller than that of the matrix, but it has a high bulk modulus k_{ru} when there isn't debonding or cavitation. So, we only need to consider the uniform radial stress $\bar{\sigma}^0_{RR}$. Then, we have

$$\varepsilon^0_{RR}\big|_{R=a} = \frac{1}{3k_{ru}} \sigma^0_{RR}\big|_{R=a} \quad (21)$$

or in another form

$$\bar{\sigma}^0_{RR}\big|_{R=a} = \frac{1+\nu}{1-2\nu} \lambda \bar{u}^0_{RR}\big|_{R=a} \quad (22)$$

where, $k_{ru} = \frac{E_{ru}}{3(1-2\nu_{ru})} \cdot \lambda = \frac{k_{ru}}{k}$ is the ratio of bulk modulus of the rubber and matrix.

If debonding is complete or the bulk modulus of the rubber sphere is much smaller than Young's modulus of the matrix, the rubber sphere can be taken as a void, $\lambda \to 0$,

$$\bar{\sigma}^0_{RR}\big|_{R=a} = 0 \quad (23)$$

(2) As we have mentioned before, only the uniform radial stress $\bar{\sigma}^0_{RR}$ needs to be considered, so, $\bar{\sigma}^2_{RR}$ and $\bar{\tau}^2_{R\varphi}$ should be zero.

$$\bar{\sigma}^2_{RR}\big|_{R=a} = 0 \quad (24)$$

and (3)

$$\bar{\tau}^2_{R\varphi}\big|_{R=a} = 0 \quad (25)$$

Next, we consider the boundary conditions of the big sphere.

(4) The average stress of the horizontal area, or equator area, is σ_1. So that

$$\iint\limits_{A_h} \sigma_{\varphi\varphi}\Big|_{\varphi=\frac{\pi}{2},R=b} dA_h = \pi b^2\sigma_1 \tag{26}$$

where, A_h is the horizontal circle area. $dA_h = Rd\theta\, dR$.

(5) The average stress of arbitrary longitude area is σ_2. So that

$$\iint\limits_{A_v} \sigma_{\theta\theta}\, dA_v = \pi b^2\sigma_2 \tag{27}$$

where, A_v is the area of the vertical or longitude area, $dA_v = Rd\varphi\, dR$. Now, we derive the compatibility condition of the displacements.

(6) The horizontal square ABCD should keep its square shape after deformation. So, from Fig. 3a, it can be seen that the strain of the diagonal must be equal to the strain of the square. Then, we obtain

$$\varepsilon_2|_{AB} = \varepsilon_2|_{\varphi=0,R=b} \tag{28}$$

where, $\varepsilon_2|_{\varphi=0,R=b}$ is the transversal strain of the sphere, $\varepsilon_2|_{AB}$ is the strain of the square area along AB.

We also know that the vertical square ABA′B′ should keep its rectangular shape after deformation, as shown in Fig. 3b

$$\varepsilon_2|_{\varphi=\frac{\pi}{4},R=b} = \varepsilon_2|_{AB} \tag{29}$$

So, we obtain that

$$\varepsilon_2|_{\varphi=\frac{\pi}{4},R=b} = \varepsilon_2|_{\varphi=0,R=b} \tag{30}$$

where

$$\varepsilon_2|_{\varphi=\frac{\pi}{4},R=b} = \left(\frac{\sqrt{2}}{2}u_\varphi\Big|_{\varphi=\frac{\pi}{4},R=b} + \frac{\sqrt{2}}{2}u_\varphi\Big|_{\varphi=\frac{\pi}{4},R=b}\right)\Big/\left(\frac{\sqrt{2}}{2}b\right)$$

$$\varepsilon_2|_{\varphi=0,R=b} = u_\varphi|_{\varphi=0,R=b}/b$$

After substitution and simplification, we get

$$\bar{u}_R^2\big|_{R=b} = 2\bar{u}_\varphi^2\big|_{R=b} \tag{31}$$

So, we have got 6 linear equations to solve the 6 unknown parameters:

$$\begin{bmatrix} 2(1+\nu)(1-\lambda) & \frac{-2+4\nu-\lambda(1+\nu)}{(1-2\nu)\bar{a}^3} & 0 & 0 & 0 & 0 \\ 0 & 0 & -6\nu\bar{a}^2 & 2 & \frac{-4(5-\nu)}{\bar{a}^3} & \frac{12}{\bar{a}^5} \\ 0 & 0 & (7+2\nu)\bar{a}^2 & 1 & \frac{2(1+\nu)}{\bar{a}^3} & \frac{-4}{\bar{a}^5} \\ -2(1+\nu) & 2 & \frac{3}{2}(1-\bar{a}^4)(7+\nu) & 2(1-\bar{a}^2) & 2\left(\frac{1}{\bar{a}}-1\right)(1-2\nu) & 3\left(\frac{1}{\bar{a}^3}-1\right) \\ -2(1+\nu) & 2 & -\frac{3}{4}(1-\bar{a}^4)(7+\nu) & -(1-\bar{a}^2) & -\left(\frac{1}{\bar{a}}-1\right)(1-2\nu) & -\frac{3}{2}\left(\frac{1}{\bar{a}^3}-1\right) \\ 0 & 0 & 7-10\nu & 0 & -3 & \frac{2}{5} \end{bmatrix} \cdot \begin{bmatrix} \bar{A}_0 \\ \bar{D}_0 \\ \bar{A}_2 \\ \bar{B}_2 \\ \bar{C}_2 \\ \bar{D}_2 \end{bmatrix}$$

$$= \begin{bmatrix} 0 \\ 0 \\ 0 \\ (1+\nu)\frac{\sigma_1}{E} \\ (1+\nu)\frac{\sigma_2}{E} \\ 0 \end{bmatrix}$$

where, $\bar{a} = a/b$.

Simplified the above determinant, we can write in another form:

$$\begin{bmatrix} 2(1+\nu)(1-\lambda)\bar{a}^3 & \frac{-2+4\nu-\lambda(1+\nu)}{1-2\nu} & 0 & 0 & 0 & 0 \\ -2(1+\upsilon) & 2 & 0 & 0 & 0 & 0 \\ 0 & 0 & -6\nu\bar{a}^7 & 2\bar{a}^5 & -4(5-\nu)\bar{a}^2 & 12 \\ 0 & 0 & (7+2\nu)\bar{a}^7 & \bar{a}^5 & 2(1+\nu)\bar{a}^2 & -4 \\ 0 & 0 & \frac{3}{2}(7+\nu) & 2 & -2(1-2\nu) & -3 \\ 0 & 0 & 7-10\nu & 0 & -3 & \frac{2}{5} \end{bmatrix} \cdot \begin{bmatrix} \bar{A}_0 \\ \bar{D}_0 \\ \bar{A}_2 \\ \bar{B}_2 \\ \bar{C}_2 \\ \bar{D}_2 \end{bmatrix} = \begin{bmatrix} 0 \\ \frac{(1+\nu)}{3}\frac{\sigma_1+2\sigma_2}{E} \\ 0 \\ 0 \\ \frac{2(1+\nu)}{3}\frac{\sigma_1-\sigma_2}{E} \\ 0 \end{bmatrix}$$

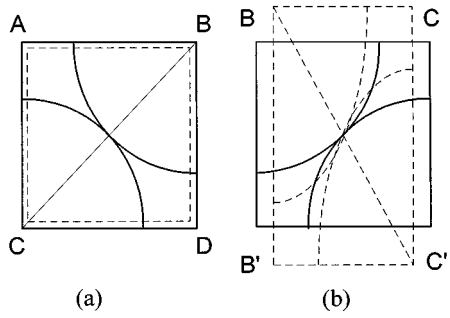

Figure 3 Displacements of the horizontal (a) and longitudinal (b) sections.

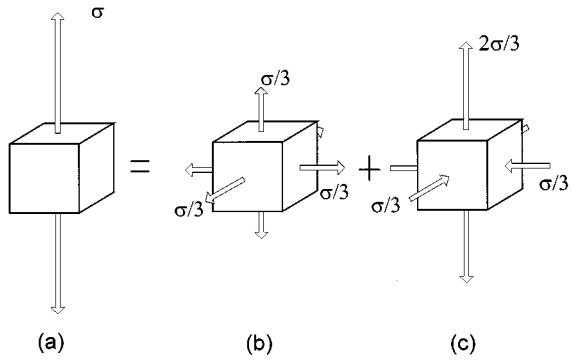

Figure 4 Macromechanical resolution of stress into two parts: dilatation stress and nondilatation stress.

We have seen that if debonding is complete or the bulk modulus of the rubber sphere is very small, the rubber sphere can be taken as a void, then $\lambda \to 0$.

$$\bar{D}_0 = \frac{-\bar{a}^{*3}(1-\lambda)(1+\nu)(1-2\nu)}{3[2(1-\bar{a}^{*3})(1-2\nu)+\lambda(1+2\bar{a}^{*3}+\nu-4\nu\bar{a}^{*3})]}\frac{\sigma}{E} \tag{33}$$

$$\bar{A}_2 = \bar{B}_2 = \bar{C}_2 = \bar{D}_2 = 0 \tag{34}$$

where $\bar{a}^{*3} = V_f$

2.2. Non-dilatation stress

The rest of the matrix can be thought of as a three-dimensional net between spheres, as shown in Fig. 2. It is well known that, the rigidity of a net is low under this kind of stress. To simplify the problem, we assume that neglecting its effect on general rigidity will not cause a significant error when the volume fraction of rubber particle is not very large. And, because of the rest of the matrix is comparatively far from the stress concentration area, we can assume the rate of its horizontal and vertical stresses to be equal to the remote stress, which means

$$\sigma_2/\sigma_1 = (-\sigma/3)/(2\sigma/3) \tag{35}$$

Then, we obtain

$$\bar{A}_0 = \bar{D}_0 = 0 \tag{36}$$

$$\bar{A}_2 = \frac{20\bar{a}^3(1-\bar{a}^2)(1+\nu)}{f(\bar{a},\nu)}\frac{\sigma^{**}}{E} \tag{37}$$

$$\bar{B}_2 = \frac{2(1+\nu)(196-126\bar{a}^5+175\bar{a}^7-420\nu+200\nu^2-25\nu^2\bar{a}^7)}{3f(\bar{a},\nu)}\frac{\sigma^{**}}{E} \tag{38}$$

Solving these function groups, we can get all the parameters,

Now, the problem that we have to discuss is that even the best-packed statistical unique sized particle spheres can only occupy 74% of the whole space. So, how can we deal with the remaining 26% of the matrix?

We can resolve the stresses into two parts, dilatation stress and non-dilatation stress. For example, the uniaxial tension can be resolved as shown in Fig. 4.

2.1. Dilatation stress

We could average the remaining 26% of matrix into spheres, which will get the same results with composite spheres' assemblage theory.

$$\bar{A}_0 = \frac{-2+4\nu-\lambda(1+\nu)}{6[2(1-\bar{a}^{*3})(1-2\nu)+\lambda(1+2\bar{a}^{*3}+\nu-4\nu\bar{a}^{*3})]}\frac{\sigma}{E} \tag{32}$$

$$\bar{C}_2 = \frac{5\bar{a}^3(1+\nu)(28+7\bar{a}^7-40\nu+5\nu\bar{a}^7)}{3f(\bar{a},\nu)}\frac{\sigma^{**}}{E} \tag{39}$$

and

$$\bar{D}_2 = \frac{2\bar{a}^5(1+\nu)(28+7\bar{a}^7-40\nu+5\nu\bar{a}^7)}{f(\bar{a},\nu)}\frac{\sigma^{**}}{E} \tag{40}$$

where,

$$\sigma^{**} = \sigma_1 - \sigma_2, \quad \bar{a}^3 = V_f/0.74,$$

and V_f is the volume fraction of rubber particle.

$$f(\bar{a},\mu) = 7(56+25\bar{a}^3-117\bar{a}^5+50\bar{a}^7-14\bar{a}^{10}) - 105\nu(8-5\bar{a}^3-3\bar{a}^5)+50\nu^2(8-8\bar{a}^3 -\bar{a}^7+\bar{a}^{10})$$

Now, we extrapolate the results of the sphere to the upper surface of the rest of the matrix (the shadow part in Fig. 2b), the stress of that is

$$\sigma_{1m} \approx \sigma_{RR}|_{R=1.4142b,\varphi=0} = \psi(\bar{a}, \nu) \cdot \sigma^{**} \quad (41)$$

where

$$\psi(\bar{a}, \nu) = \frac{\sigma_{RR}|_{R=1.4142b,\varphi=0}}{\sigma^{**}} = \left[-12\nu \frac{E}{\sigma^{**}} \bar{A}_2 + 2\frac{E}{\sigma^{**}} \bar{B}_2 - \sqrt{2}(5-\nu)\frac{E}{\sigma^{**}} \bar{C}_2 + \frac{3}{2}\sqrt{2}\frac{E}{\sigma^{**}} \bar{D}_2 \right] \Big/ (1+\nu) \quad (42)$$

can be easily obtained from Equation 36 to Equation 40. Now, σ^{**} is still unknown. Then, from the equation of equilibrium, it can be obtained that

$$\frac{2}{3}\sigma^{**}\frac{\pi}{2}b^2 + \psi(\bar{a}, \nu)\cdot\sigma^{**}\left(2-\frac{\pi}{2}\right)b^2 = \frac{2}{3}\sigma \cdot 2b^2 \quad (43)$$

And, we get

$$\sigma^{**} = \sigma \Big/ \left[\frac{\pi}{4} + 1.5\psi(\bar{a}, \nu) \cdot \left(1 - \frac{\pi}{4}\right) \right] \quad (44)$$

After substitution, we have

$$\sigma^{**} = \frac{f(\bar{a}, \nu)}{g(\bar{a}, \nu)}\sigma \quad (45)$$

where

$$g(\bar{a}, \nu) = [392 + 31.22\bar{a}^3 - 659.1\bar{a}^5 + 350\bar{a}^7 - 94\bar{a}^{10}] + \nu[-840 + 508.1\bar{a}^3 + 270\bar{a}^5 - 6.8\bar{a}^{10}] + \nu^2[400 - 344.5\bar{a}^3 - 50\bar{a}^5 + 43\bar{a}^{10}]$$

After superposition, in general, it can be obtained that

$$\bar{A}_0 = \frac{-2 + 4\nu - \lambda(1+\nu)}{6[2(1-V_f)(1-2\nu) + \lambda(1 + 2V_f + \nu - 4\nu V_f)]}\frac{\sigma}{E} \quad (46)$$

$$\bar{D}_0 = \frac{-V_f(1-\lambda)(1+\nu)(1-2\nu)}{3[2(1-V_f)(1-2\nu) + \lambda(1 + 2V_f + \nu - 4\nu V_f)]}\frac{\sigma}{E} \quad (47)$$

$$\bar{A}_2 = \frac{20\bar{a}^3(1-\bar{a}^2)(1+\nu)}{g(\bar{a}, \nu)}\frac{\sigma}{E} \quad (48)$$

$$\bar{B}_2 = \frac{2(1+\nu)(196 - 126\bar{a}^5 + 175\bar{a}^7 - 420\nu + 200\nu^2 - 25\nu^2\bar{a}^7)}{3g(\bar{a}, \nu)}\frac{\sigma}{E} \quad (49)$$

$$\bar{C}_2 = \frac{5\bar{a}^3(1+\nu)(28 + 7\bar{a}^7 - 40\nu + 5\nu\bar{a}^7)}{3g(\bar{a}, \nu)}\frac{\sigma}{E} \quad (50)$$

$$\bar{D}_2 = \frac{2\bar{a}^5(1+\nu)(28 + 7\bar{a}^7 - 40\nu + 5\nu\bar{a}^7)}{g(\bar{a}, \nu)}\frac{\sigma}{E} \quad (51)$$

where $\bar{a}^3 = V_f/0.74$, and the formula of g$(\bar{a}, \nu)$ can be simplified numerically as follows

$$g(\bar{a}, \nu) \approx 392 - 884.7\bar{a}^6 + 718\bar{a}^9 + \nu(-840 + 548\bar{a}^3 + 260\bar{a}^6) + \nu^2(400 - 354\bar{a}^3)$$

Then, the stresses and displacements can be determined.

3. Results and discussion

The material property can be chosen as following: Young's modulus of the matrix is 3.5 GPa and Poisson's ratio of matrix is 0.35.

(1) The bulk modulus of the rubber sphere is chosen as 0.067 GPa.

We choose this value in order to compare with previous results, which used a low bulk modulus. In this case, the rubber sphere can be, in fact, thought of as a void. This may happen when the rubber sphere is debonded.

Fig. 5 gives the Young's modulus and Poisson's ratio of the material. It can be seen that our results fit very well with the results obtained by FEM using either a cylinder model or a 3-D model, especially when the volume fraction is not quite large.

Fig. 6 shows the maximum Von Mises stress concentration factors. It can be seen that our results agree well with that of the cylinder model, but are relatively smaller than that of the 3-D model, although the difference is still in the acceptable range of engineering. This is possibly caused by the axisymmetric assumption in our model or in the cylinder model. But, this difference is also due to the fact that the elements of the Chen and Mai's 3-D model is not small enough, especially at the places where the Von Mises stress should have the maximum value. Based on their model, the elements at such places are even rougher than at other places. Fig. 6b shows the maximum stress concentration factors about $\sigma_{\varphi\varphi}$. It can be seen that our results also have a good agreement with that of the cylinder model.

Table I gives more results about Von Mises stress concentration factors.

(2) The bulk modulus of the rubber sphere is chosen as 2 GPa.

This is the typical bulk modulus of the rubber [4]. Fig. 7 shows the Young's modulus and Poission's ratio of the material. It can be seen that our results fit very well with both experimental observation and results

TABLE I Von Mises stress concentration factors

$\bar{R}\backslash\varphi^0$	0	15	30	45	60	75	90
			(a) $\bar{a} = 0.1$ or $V_f = 0.074\%$				
0.1	0.79316	0.67277	0.50830	0.82110	1.3699	1.8043	1.9661
0.12	0.27426	0.42616	0.69115	0.94602	1.1520	1.2856	1.3319
0.2	0.65222	0.75018	0.93057	1.05334	1.07522	1.03214	1.00285
1	0.99868	0.99951	1.00127	1.00254	1.00249	1.00161	1.00112
			(b) $\bar{a} = 0.5$ or $V_f = 9.25\%$				
0.5	0.78998	0.66476	0.48936	0.81332	1.37482	1.81684	1.98126
0.6	0.32012	0.45526	0.7085	0.96151	1.1705	1.308	1.35598
0.8	0.57307	0.72562	0.9846	1.15834	1.20223	1.16226	1.13148
1	0.89507	0.97847	1.13892	1.247	1.2549	1.19929	1.16466
			(c) $\bar{a} = 0.7$ or $V_f = 25.4\%$				
0.7	1.17717	1.00146	0.68552	0.97748	1.68592	2.26097	2.47598
0.8	0.66963	0.69985	0.85002	1.15049	1.50057	1.77155	1.87264
0.9	0.68688	0.84292	1.14066	1.4008	1.56691	1.64604	1.66733
1	0.87221	1.04167	1.35109	1.57863	1.66152	1.64466	1.62209
			(d) $\bar{a} = 0.8$ or $V_f = 37.9\%$				
0.8	1.77549	1.52824	1.03805	1.28955	2.21552	2.99516	3.28852
0.85	1.32035	1.17339	0.97811	1.32575	2.03619	2.62698	2.84993
0.9	1.10693	1.0831	1.1552	1.50807	2.01113	2.42223	2.5779
1	1.06544	1.21432	1.53645	1.86377	2.11519	2.26607	2.31558

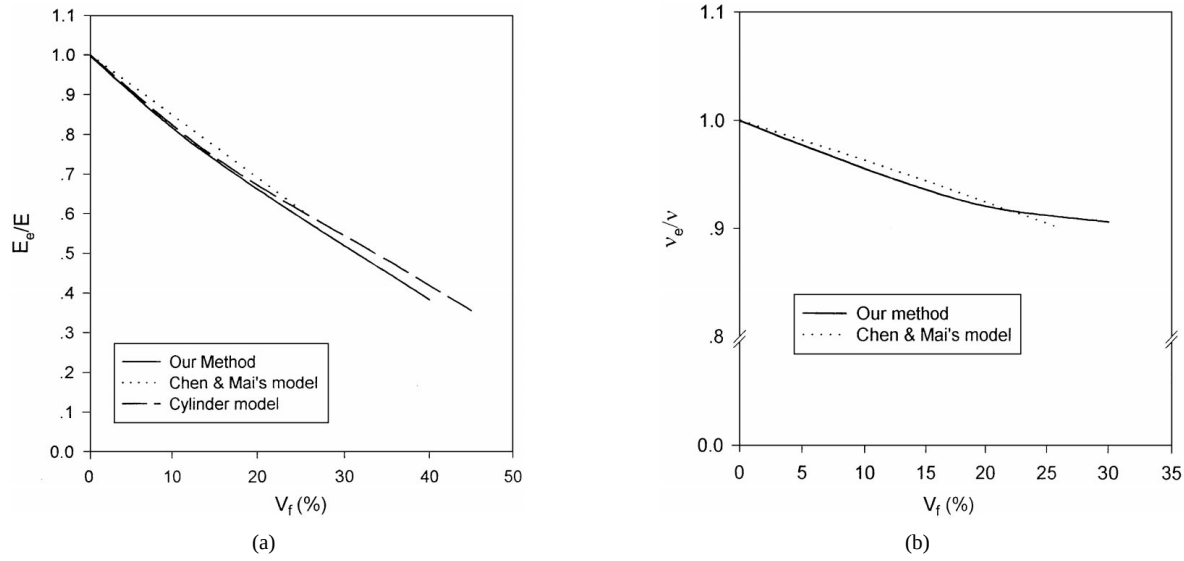

(a) (b)

Figure 5 Young's modulus (a) and Poisson's ratio (b) of the composite material with low bulk modulus ratio $\lambda = 0.017$.

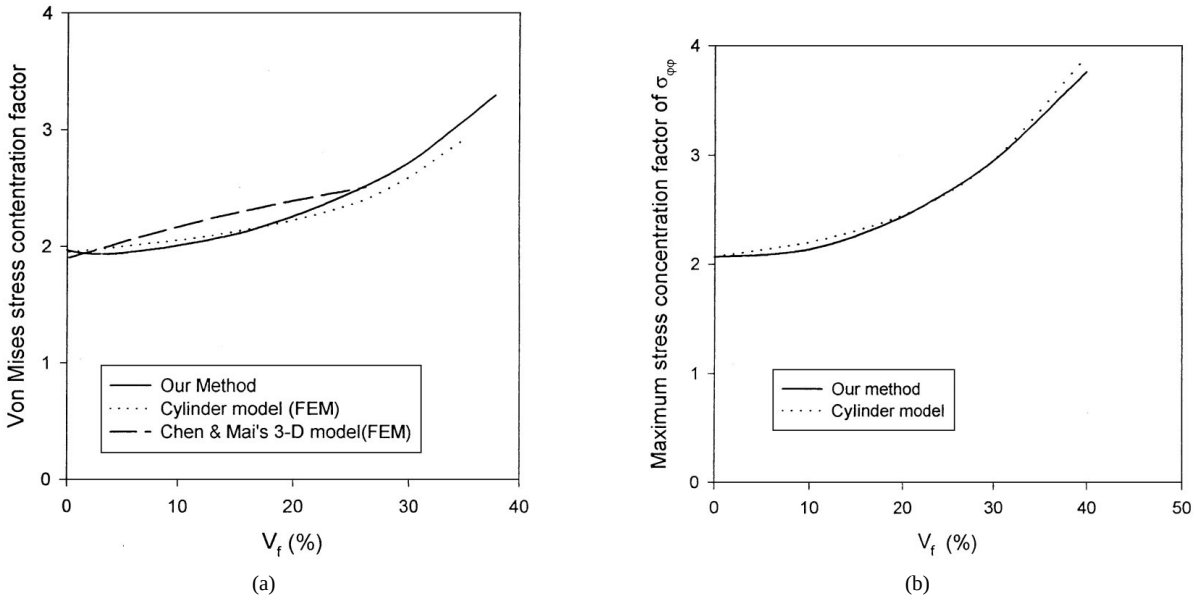

(a) (b)

Figure 6 Stress concentration factors of the composite material with low bulk modulus ratio $\lambda = 0.017$: (a) The maximum Von Mises stress concentration factors; (b) The maximum stress concentration factors about $\sigma_{\varphi\varphi}$.

TABLE II Von Mises stress concentration factors

$\bar{R}\backslash\varphi^0$	0	15	30	45	60	75	90
			(a) $\bar{a} = 0.1$ or $V_f = 0.074\%$				
0.1	1.17174	1.04823	0.79848	0.82990	1.23551	1.62432	1.77504
0.12	0.49335	0.57026	0.74437	0.93786	1.10448	1.21588	1.25497
0.2	0.69955	0.78737	0.95110	1.05964	1.06962	1.01723	0.98405
1	0.99906	0.99985	1.00151	1.00263	1.00244	1.00146	1.00093
			(b) $\bar{a} = 0.5$ or $V_f = 9.25\%$				
0.5	1.21485	1.08635	0.81702	0.81595	1.2127	1.60351	1.7556
0.6	0.56599	0.6276	0.77666	0.95346	1.11266	1.22205	1.26094
0.8	0.67680	0.80093	1.02188	1.16693	1.18764	1.12953	1.09113
1	0.94818	1.02226	1.16477	1.25548	1.24806	1.1803	1.1406
			(c) $\bar{a} = 0.7$ or $V_f = 25.4\%$				
0.7	1.71148	1.53289	1.13123	1.01564	1.47806	1.9792	2.17696
0.8	1.02757	1.00877	1.01621	1.15605	1.40257	1.62365	1.71024
0.9	0.93827	1.03384	1.23376	1.41273	1.51699	1.55507	1.56158
1	1.05548	1.18236	1.42409	1.59498	1.63151	1.57979	1.54325
			(d) $\bar{a} = 0.8$ or $V_f = 37.9\%$				
0.8	2.4339	2.18373	1.60823	1.38171	1.97283	2.65145	2.92151
0.85	1.86927	1.70592	1.37686	1.3729	1.86051	2.37111	2.57405
0.9	1.56936	1.50227	1.41344	1.53731	1.88665	2.22747	2.3635
1	1.40255	1.48569	1.67991	1.888	2.04802	2.14106	2.17065

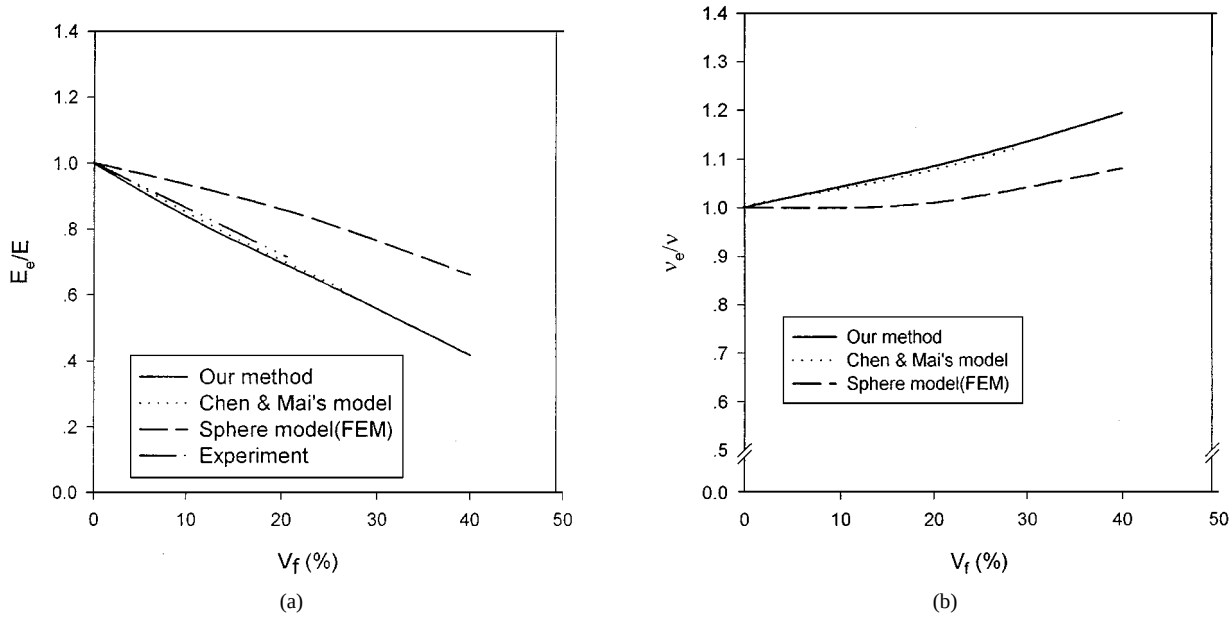

Figure 7 Young's modulus (a) and Poisson's ratio (b) of the composite material with bulk modulus ratio $\lambda = 0.5$.

obtained by FEM using either a cylinder model or a 3-D model. But, the FEM results obtained by a simple sphere model are quite different from the other results. The inaccuracy of this simple sphere model may be caused by the complete neglect of the remaining 26% of the matrix or, in another word, average them into spheres.

Fig. 8 gives the maximum Von Mises stress concentration factors. It can be seen that our results are a little smaller than those of the 3-D model, but the difference is still in the acceptable range of engineering. As we mentioned before, this may be caused not only by the axisymmetric assumption in our method or the cylinder model, but also by the fact that the elements of the Chen and Mai's 3-D model are not small enough. However, both works show similar results and they are proven to be right.

Table II gives out more results about Von Mises stress concentration factors.

It can be seen, from both Table I and Table II, that the largest Von Mises stress always appears first at the 90° of the rubber sphere surface or, in another word, at the equator of the rubber sphere surface. When the volume fraction is of medium value such as 9.25% or 25.4% or case (b) and case (c) in Table I, we find that the largest Von Mises stress gradually turned to about 45° when the radius R increases. This conclusion fits well with FEM analysis [7] and experimental observation of shear bands [11]. An interesting finding is, when the volume fraction is quite large such as 37.9%, the largest Von

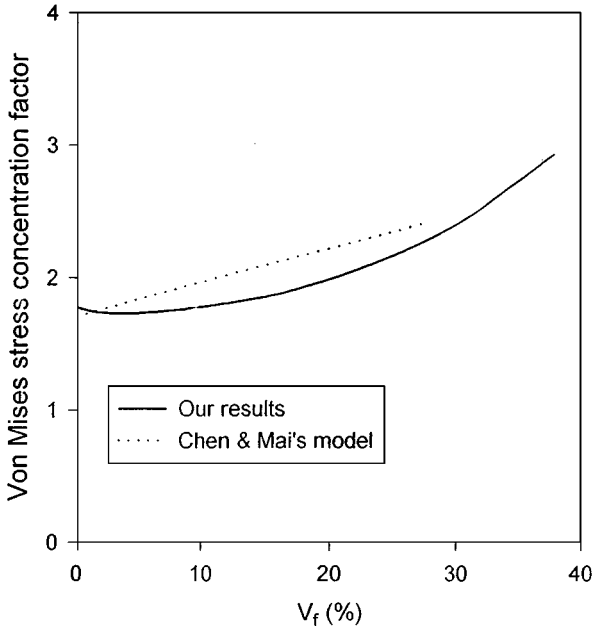

Figure 8 The maximum Von Mises stress concentration factors of the composite material with bulk modulus ratio $\lambda = 0.5$.

Mises stress stays close to 90 ° when R increases. When the volume fraction is very small such as 0.074% and as R increases, the largest Von Mises stress first appears at 90 °, and then turns to 45 °. Then, Von Mises stress gradually becomes almost the same at every degree.

4. Conclusion

It can be seen that our predicted results fit quite well with the experimental measurement of material properties and have nice agreement with previous FEM analysis results of stress concentration factors. Of course, the previous FEM analyses also have disadvantages, as we have mentioned in part of introduction. But, if there is a nice agreement with the results of theoretical and FEM analyses, they can prove each other to be basically right. So, the assumptions introduced in this analysis are proved to be acceptable.

And, comparing with FEM analysis, the analytical method is quite simple, needing only to solve a linear function group with 6 unknown parameters, and formula are given out. So, it can be easily used to calculate a huge amount of results and to understand the deformation mechanisms to fit the requirements of engineering.

It can be seen that the largest Von Mises stress always first appears at the 90 ° of rubber sphere surface or, in another word, at the equator of rubber sphere surface. When volume fraction is of medium value, as radius R increases, the largest Von Mises stress gradually turned to about 45 °. This conclusion fits well with FEM analysis and experimental observation of shear bands. An interesting found is when the volume fraction is quite large, the largest Von Mises stress nearly keep at 90 ° when R increase. But, when the volume fraction is very small, as R increases, the largest Von Mises stress first appears at the 90 °, then turns to 45 °. Then, gradually Von Mises stress become almost same at every degree. This analysis may imply the explanation of shear band in damage initiation for rubber toughened polymers. But, of course, further plastic analyses are needed to prove the inference.

Considering more parameters may gave a more accurate analysis. This work is now in process.

Acknowledgements

The authors wish to acknowledge the financial support of the Korean Research Foundation made in the Program Year 1997.

References

1. F. LU, W. J. CANTWELL and H. H. KAUSCH, *J. of Mater. Sci.* **32** (1997) 3055–3059.
2. M. SCHNEIDER, T. PITH and M. LAMBLA, *ibid.* **32** (1997) 5991–5204.
3. B. BUCKNALL, F. F. P. COTE and I. K. PARTRIDGE, *ibid.* **21** (1986) 301–306.
4. A. LAZZERI and C. B. BUCKNALL, *ibid.* **28** (1993) 6799–6808.
5. A. F. YEE and R. A. PEARSON, *ibid.* **21** (1986) 2462–2474.
6. F. J. GUILD and R. J. YOUNG, *ibid.* **24** (1989) 2454–2460.
7. Y. HUANG and A. J. KINLOCH, *ibid.* **27** (1992) 2753–2762.
8. A. C. STEENBRINK and E. VAN DER GIESSEN, *Journal of Engineering Materials and Technology* **119** (1997) 256–261.
9. F. J. GUILD and A. J. KINLOCH, *J. Mater. Sci. Lett.* **13** (1994) 629–632.
10. X.-H. CHEN and Y.-W. MAI, *Key Engineering Materials* **145–149** (1998) 233–242.
11. A. SURVEY, *Journal of Applied Mechanics* **50** (1983) 481–505.
12. I. JASIUK, P. Y. SHENG and E. TSUCHIDA, *ibid.* **64** (1997) 471–479.
13. T. K. CHEN and Y. H. JAN, *J. of Mater. Sci.* **27** (1992) 111–121.
14. R. W. LITTLE, "Elasticity" (Prentice-Hall, New Jersey, 1973).

Received 18 June 1998
and accepted 5 May 1999